Proc. Int. Conf. Strongly Correlated Electron Systems (SCES2019)
JPS Conf. Proc. **30**, 011029 (2020)
https://doi.org/10.7566/JPSCP.30.011029

Inter-grain Phase Transitions in Superconducting Ceramic $YBa_2Cu_3O_{7-\delta}$ under Low Magnetic Fields

Hiroyuki DEGUCHI[1*], Takanori FUJII[1], Yuki KATO[1], Masaki MITO[1], Akihiko HISADA[2], Kuniyuki KOYAMA[2], and Makoto HAGIWARA[3]

[1]*Faculty of Engineering, Kyushu Institute of Technology, Kitakyushu 804-8550, Japan*
[2]*Graduate School of Technology, Industrial and Social Sciences, Tokushima University, Tokushima 770-8506, Japan*
[3]*Department of Electronics, Kyoto Institute of Technology, Kyoto 606-8585, Japan*

**E-mail: deguchi@mns.kyutech.ac.jp*

(Received September 14, 2019)

We investigated the magnetic field dependence of inter-grain phase transitions in the ceramic $YBa_2Cu_3O_{7-\delta}$. To this end, we measured the temperature dependences of the nonlinear magnetic responses and the current-voltage characteristics under low magnetic fields. We then estimated the inter-grain temperatures of the glass and superconducting transitions. The field-temperature phase diagram of the inter-grain ordering was similar to that of $YBa_2Cu_4O_8$ ceramic. The results imply the occurrence of chiral-glass ordering in ceramic cuprate superconductors under low magnetic fields.
.

KEYWORDS: Ceramic superconductor, $YBa_2Cu_3O_{7-\delta}$, Chiral glass, Inter-grain ordering, Phase diagram

1. Introduction

Granular superconductors with *d*-wave symmetry, such as cuprate superconductors composed of sub-micron grains, are considered as random Josephson-coupled networks of 0 and π junctions. A circulating local supercurrent and a magnetic flux are generated spontaneously when an odd number of π junctions exist in a closed loop of superconducting grains. Kawamura and Li [1] predicted that the frustration effect caused by the random distribution of π junctions leads to a chiral-glass state in granular cuprate superconductors. In experimental studies, ceramic superconductors with weak Josephson couplings, for instance$YBa_2Cu_4O_8$ [2,3] and $YBa_2Cu_3O_{7-\delta}$ [4,5], have shown successive phase transitions under a zero magnetic field. As the temperature decreases, the first phase transition of each grain, identified as the intra-grain superconducting ordering with a small diamagnetism induced by the Meissner effect, occurs at T_{c1}. Usually, T_{c1} coincides with the bulk superconducting transition temperature T_c. The second phase transition is the inter-grain glass transition at T_{c2}, where a sharp peak of nonlinear magnetic response is found [2]. The inter-grain glass transition at T_{c2} suggests the onset of the chiral-glass phase, a magnetic-glass state with a small but nonzero resistivity [6]. At the chiral-glass transition T_{c2}, the chirality is frozen, i.e., the circulation of superconducting current loops is frozen in a Josephson-coupled network.

The third transition at T_{c3} is the inter-grain superconducting transition, where the phases of the superconducting order parameter of inter-grains are frozen and the system becomes a true superconductor [6]. Experimentally, this transition is observed as the onset of zero resistivity. However, in our previous studies on the ceramic $YBa_2Cu_4O_8$ [3] and $YBa_2Cu_3O_{7-\delta}$ [4], T_{c3} was difficult to estimate because the change in the linear resistivity was very slight and the inter-grain superconducting phase could not be confirmed.

In this study, we measured the temperature dependence of the nonlinear magnetic response of the ceramic $YBa_2Cu_3O_{7-\delta}$ and obtained the current-voltage (*I-V*) curves under varying magnetic fields. From the results, we estimated the field dependences of T_{c2} and T_{c3}. We also experimentally obtained the magnetic field dependence of inter-grain phase transitions. The field-temperature phase diagram of the inter-grain ordering was compared with that of the ceramic $YBa_2Cu_4O_8$ [7] and the results of Monte Carlo simulations [6].

2. Experiments

The ceramic $YBa_2Cu_3O_{7-\delta}$ sample was prepared as follows [4,5]. Well mixed sub-micron size powders prepared by the coprecipitation method were calcined at 840 °C for 24 h in air and sintered under the same conditions as the calcinations. The sample was annealed at 500 °C for 12 h in an O_2 flow. The DC and AC magnetizations were measured with a SQUID magnetometer (Quantum Design MPMS-XL7) using the ultra-low-field option. The sample space of the magnetometer was shielded with μ-metal, which reduced the residual field to less than 10 mOe. The nonlinear magnetic response was derived from the third-harmonic in-phase Fourier component of the AC-field response. The linear resistivity and *I-V* characteristics were measured by a conventional four-terminal method using a combined current source (KEITHLEY 6221) and a nanovoltmeter (KEITHLEY 2182A). The transport probe with four-terminal connecters was inserted into the sample room of the SQUID measurement system (MPMS-XL7), which controls the temperature and the magnetic field. To eliminate the

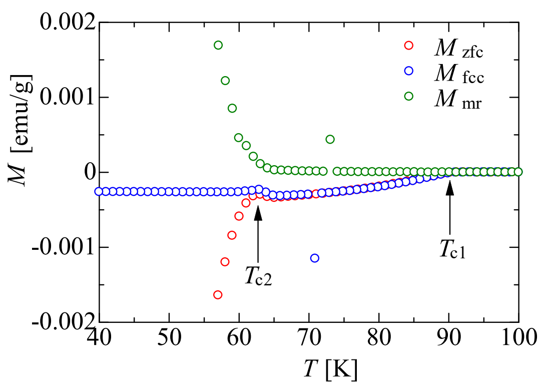

Fig. 1. Temperature dependences of the zero-field-cooled magnetization M_{zfc}, the field-cooled magnetization M_{fcc}, and the thermoremanent magnetization M_{mr} at H= 0.5 Oe

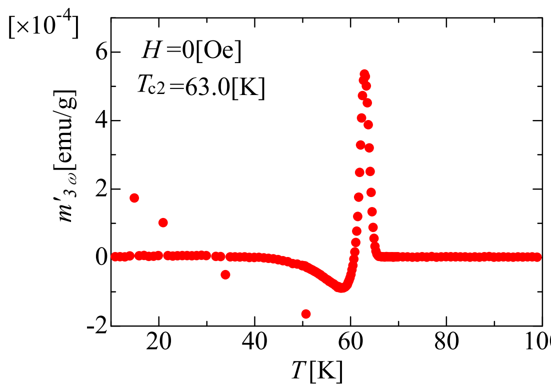

Fig. 2. Temperature dependence of the nonlinear magnetic response $m'_{3\omega}$ at 1.0 Hz. The AC field amplitude was 0.1 Oe at H = 0 Oe

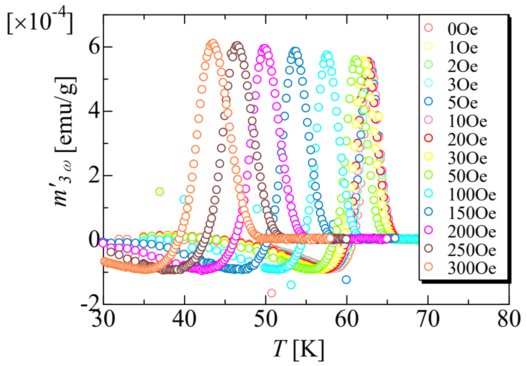

Fig. 3. Temperature dependence of the nonlinear magnetic response $m'_{3\omega}$ under various applied fields (H = 0-300 Oe)

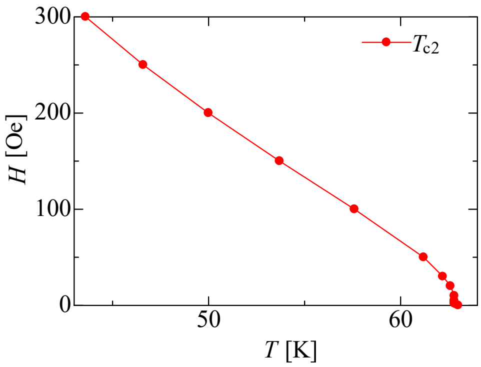

Fig. 4. Magnetic field dependence on T_{c2} estimated from the peak temperatures of $m'_{3\omega}$ in Fig. 3

constant thermoelectric voltage and minimize the power dissipated in the sample, we applied the delta method for low-voltage measurements. The external magnetic field was applied perpendicularly to the DC current.

3. Results

From the measured DC magnetizations, we determined the transition temperatures T_{c1} and T_{c2} under an applied magnetic field H = 0.5 Oe. Figure 1 shows the temperature dependences of the zero-field-cooled, field-cooled, and thermoremanent magnetizations. The small diamagnetism due to the Meissner effect in each $YBa_2Cu_3O_{7-\delta}$ grain appeared at T_{c1} = 90 K in the zero-field-cooled, and field-cooled magnetizations. The zero-field-cooled magnetization steeply branched from the field-cooled one at the inter-grain glass transition temperature T_{c2} = 63 K. This branching temperature coincides with the vanishing point of the thermoremanent magnetization, which must be caused by the release of magnetic flux trapped in the closed loops in the ceramics.

The nonlinear magnetic response $m'_{3\omega}$ was estimated by measuring the third-harmonic in-phase Fourier component of the AC-field response at 1.0 Hz. Here, the AC field amplitude was set to 0.1 Oe. Figure 2 plots the temperature dependence of $m'_{3\omega}$ in the absence of an applied field. The $m'_{3\omega}$ peaked at T_{c2} = 63.0 K, the chiral-glass transition of the ceramics under zero applied field [2]. Figure 3 shows the temperature dependences of $m'_{3\omega}$ as the magnitude of the applied field ranged from 0 to 300 Oe, and Figure 4 plots the magnetic field as a function of T_{c2}, estimated from the peak temperature of $m'_{3\omega}$ under an applied field. The $m'_{3\omega}$ peak shifted only marginally as the field increased from 0 to 30 Oe, but remarkably shifted toward lower temperatures as the field increased above 300 Oe.

Next, we measured the temperature dependence of the linear resistivity ρ_0 at an applied DC current of 1.0 mA. The zero-field dependence of ρ_0 on temperature is shown in Figure 5. As the temperature lowered, ρ_0 decreased rapidly at T_{c1}, and then decreased monotonously to almost zero around T_{c2}. The temperature dependence of ρ_0 around T_{c2}

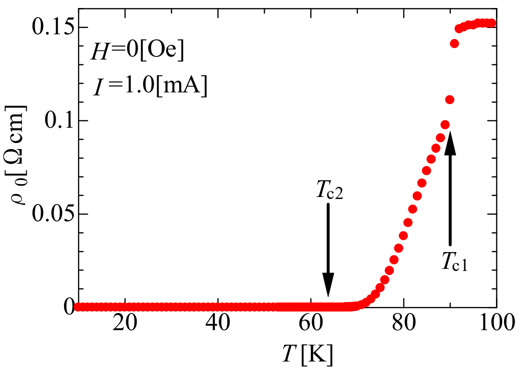

Fig. 5. Temperature dependence of the linear resistivity ρ_0, measured at a DC current of 1.0 mA in the absence of a magnetic field

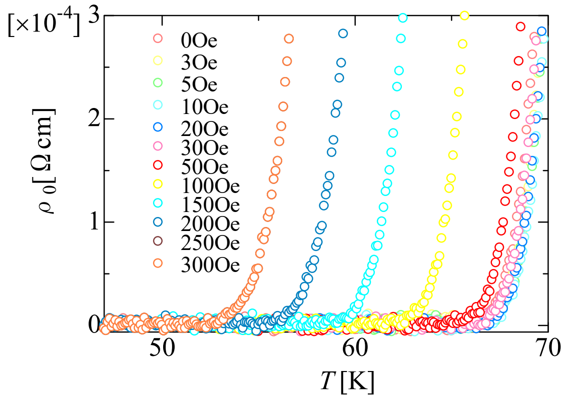

Fig. 6. Temperature dependence of ρ_0 around T_{c2} under different applied fields (H = 0-300 Oe). The DC current is 1.0 mA.

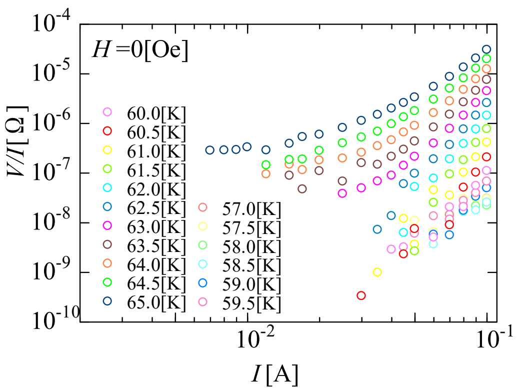

Fig. 7. Nonlinear resistivity V/I versus current around T_{c3} at H = 0 Oe and various temperatures

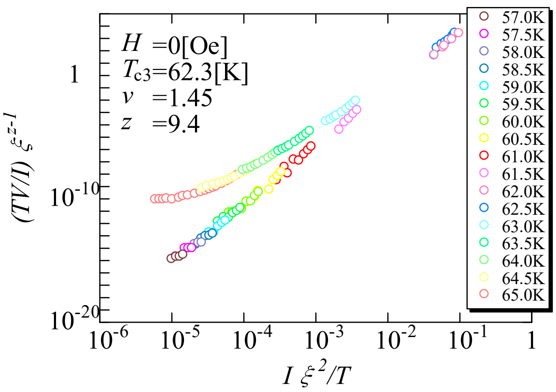

Fig. 8. Scaling plot of the data in Fig.7, obtained by adjusting the parameters: T_{c3} = 62.3 K, ν = 1.45, and z = 9.4

under different applied fields is shown in Figure 6. The temperature at which ρ_0 almost vanished shifted leftward (toward 0 K) with increasing field. The transition temperature T_{c3} at $\rho_0 = 0$ is difficult to measure because ρ_0 diminishes continuously with decreasing temperature. Therefore, we measured the I-V curves and estimated T_{c3} from the nonlinear resistivity versus current curves. The inter-grain superconducting transition temperature T_{c3} was then determined by dynamic scaling analysis [8]. Granato numerically studied the resistivity behavior of inhomogeneous superconductors with random π junctions [8], and found a resistive inter-grain transition in the chiral-glass phase at finite temperatures. He similarly estimated the critical exponents by dynamic scaling analysis. Figure 7 shows the current dependence of the nonlinear resistivity V/I at $H = 0$ Oe in the temperature range between 57-65 K. At high temperatures ($T > 63$ K), the V/I tended to a small but finite value as the current I decreased. At lower

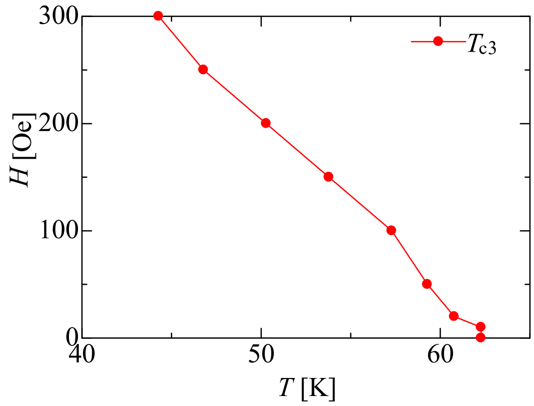

Fig. 9. Magnetic field dependence of T_{c3} estimated in the dynamic scaling analysis of nonlinear resistivity (see Figure 8)

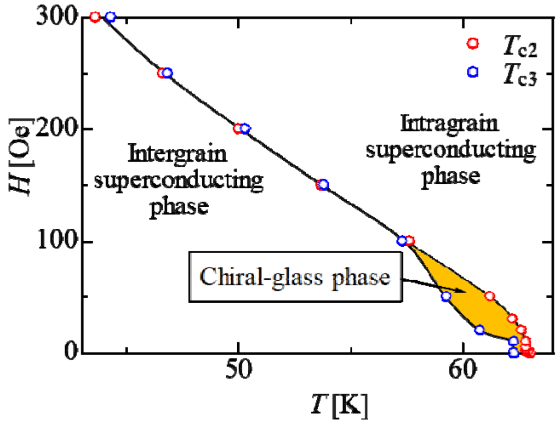

Fig. 10. Phase diagram of the ceramic $YBa_2Cu_3O_{7-\delta}$ superconductor

temperature (T < 62 K), the V/I became vanishingly small with decreasinf I. The inter-grain superconducting transition can be confirmed by scaling the nonlinear resistivity [9]. Near the transition at T_{c3}, the parametet scaled as $\xi \propto |T\text{-}T_{c3}|^{-\nu}$ and the relaxation time scaled as $\tau \propto \xi^z$, where ν and z are the corrlation length and dynamical critical exponent, respectively. The nonlinear resistivities should then scale as $TV\xi^{z-1}/I = g_{\pm}(I\xi^2/T)$ where $g(x)$ is a scaling function [9]. The + and – signs denote $T > T_{c3}$ and $T < T_{c3}$, respectively. Figure 8 is the scaling plot of the data in Figure 7, obtained by adjusting the parameters with $T_{c3} = 62.3$ K, $\nu = 1.45$, and $z = 9.4$. The upper curve plots the data above T_{c3} and corresponds to the scaling function $g_+(I\xi^2/T)$, whereas the lower curve plots the data below T_{c3} and corresponds to $g_-(I\xi^2/T)$. We also measured the current dependence of the nonlinear resistivity while varying the magnetic field from 0 to 300 Oe, and estimated T_{c3} at each magnetic field from the dynamic scaling analysis. The resulting plots were similar to Figure 8 for $H = 0$ Oe. Figure 9 shows the magnetic field dependence of T_{c3}. The field dependence of T_{c3} differed from that of T_{c2} under low magnetic fields (H < 100 Oe), but converged to that of T_{c2} under higher fields (H > 100 Oe).

4. Discussion and conclusions

The magnetic field dependences of the transition temperatures T_{c2} and T_{c3} were estimated from the measured the nonlinear magnetic responses and the I-V curves, respectively. Figure 10 shows the field-temperature phase diagram of the ceramic $YBa_2Cu_3O_{7-\delta}$. The transition temperatures T_{c2} and T_{c3} divided the phase diagram into three phases: the intra-grain superconducting phase, the chiral-glass (inter-grain glass) phase, and the inter-grain superconducting phase. In the absence of a magnetic field, the temperature of chiral-glass ordering and inter-grain superconducting ordering were almost identical ($T_{c2} \simeq T_{c3}$). However, under magnetic fields below H = 50 Oe, the two ordering temperatures were decoupled, and the chiral-glass phase appeared between the inter-grain and the intra-grain superconducting phases. When the applied field exceeded H = 100 Oe, the transition line of T_{c2} coincided with that of T_{c3}, and the chiral-glass phase was absent.

Kawamura predicted a chiral-glass phase in the ordering of granular cuprate superconductors with *d*-wave symmetry in zero and applied fields [6]. In the theoretical phase diagram, the chiral-glass phase is stable under the zero magnetic field. As the field increases, the chiral-glass transition temperature should fllow the Gabay-Toulouse line of the mean-field model, and the chiral-glass phase should disappear in high magnetic field [6].

The experimentally determined phase diagram of the ceramic $YBa_2Cu_4O_8$ [7] was similar to that of the ceramic $YBa_2Cu_3O_{7-\delta}$, except for the field dependence of the chiral-glass transition temperature T_{c2} under low magnetic field. In both ceramics, chiral-glass ordering and inter-grain superconducting ordering occurred at very similar temperatures under the zero field. These orderings were decoupled in low fields and were intercepted by the chiral-glass phase between the intra-grain and the inter-grain superconducting phases.

In our previous studies on the ceramic $YBa_2Cu_4O_8$ [3] and $YBa_2Cu_3O_{7-\delta}$ [4], the linear resistivity remained at a finite value at T_{c2} and had the constant value below T_{c2} without vanishing at zero magnetic field. In the both cases, the inter-grain superconducting transition temperature T_{c3} could not be estimated by the usual resistivity measurement. In this work, we measured the *I-V* curves and estimated T_{c3} by the dynamic scaling analysis. The inter-grain superconducting phase was observed, which was not consistent with the previous results.

In conclusion, we investigated the magnetic field dependence of the inter-grain phase transitions and discussed the phase diagram of the ceramic $YBa_2Cu_3O_{7-\delta}$. The inter-grain transitions under zero and finite fields in the ceramic $YBa_2Cu_3O_{7-\delta}$ behaved similarly to those in the ceramic $YBa_2Cu_4O_8$. The results confirmed a chiral-glass phase in the granular cuprate superconductors under low magnetic fields.

References

[1] H. Kawamura and M. S. Li: Phys. Rev. Lett. **78**, 1556 (1997).
[2] M. Matsuura, M. Kawachi, K. Miyoshi, M. Hagiwara and K. Koyama: J. Phys. Soc. Jpn. **65**, 4540 (1995)
[3] H. Deguchi, D. Nawa, Y. Hashimoto, M. Mito, S. Takagi, M. Hagiwara and K. Koyama: J. Phys. Conf. Series **150**, 052043 (2009).
[4] H. Deguchi, Y. Hashimoto, T. Shoho, M. Mito, S. Takagi, K. Koyama and M. Hagiwara: Physica C 470, S834 (2010).
[5] K. Koyama, H. Houda, H. Amano, T. Saito, H. Sugawara, K. Magishi, H. Deguchi and S. Takagi: J. Phys. Soc. Jpn. **76** Supp. A, 116 (2007).
[6] H. Kawamura, J. Phys. Soc. Jpn. **79**, 011007 (2010)
[7] H. Deguchi, R. Warabino, S. Ka, M. Mito, M. Kagiwara and K. Koyama: J. Phys. Conf. Series **871**, 012011 (2017).
[8] E. Granato: Phys. Rev. B **69**, 012503 (2004).
[9] D.S. Fisher, M.P.A. Fisher, and D.A. Huse: Phys. Rev. B **43**, 130 (1991).